

# Simulations of Interleaving Two Switched-Inductor Hybrid DC Boost Converters For Fuel Cell Applications

Umar T. Shami<sup>1</sup> and Tabrez A. Shami<sup>2</sup>

<sup>1</sup> University of Engineering and Technology, Lahore, Pakistan.

<sup>2</sup> University of Central Punjab, Lahore, Pakistan.

## Abstract

This research paper introduces the interleaving of two switched-inductor hybrid units for increasing output DC voltage of a DC converter. The benefits of the proposed converter include high DC voltage gain and reduced ripple current. The proposed converter operates in four modes, working of all the four modes are discussed. A conventional method of controlling the proposed converter is adopted. Simulated steady state analysis including waveforms of converter input current, inductor current and voltages, power electronics switching device current and voltages, output load current and voltages are presented. Results show that the proposed converter demonstrates the maximum efficiency of approximately 85% at a duty ratio of 0.4.

## Index Terms

Energy Conversion, Fuel Cells, Energy System Modeling, DC-DC Power Conversion, Interleaved Step-Up Dc Converter, Switched-Inductor Step-Up Dc Converter.

## 1. INTRODUCTION

Wing to the overwhelming applications of fuel cells (FC), electrical engineers and researchers have contributed remarkable research in this area. The major research areas include portable power, transportation, and connection of FCs to distribution-grid (distributed generation). An inherent characteristic of a typical FC is that it generates low DC output load voltage [1], which is usually less than the voltage required for DC-link voltages. Therefore, FCs are used in various applications by means of a DC step-up boost converter. One disadvantage of conventional DC boost converter is that the filter-capacitor is normally large to reduce the ripple current. Another problem is that the output load voltage is sensitive to duty ratio  $D$ , especially when this ratio ranges from 0.5 to 1 [2].

Isolated DC boost converters equipped with power transformers are normally bulky in volume. The parasitic inductance of the transformer cause efficiency degrading factors such as unavoidable voltage burden, excessive transient current, conduction losses during the turning on and off the power electronics switching element, and electromagnetic interference (EMI) [3]. Conventional DC converters employing coupled-inductors or flyback transformers, comfortably step up output voltage, nevertheless the leakage inductance of the coupled inductor causes high voltage stress and decreases the efficiency [4]. Techniques have been proposed to resolve the above mentioned problems [5]–[11]. Interleaved DC boost converters include features such as output load current

ripple minimization, inductor size reduction, and uniform heat dissipation [5]–[8].

The switched-inductor hybrid circuit technique as presented by Axelrod et al. [10], provides an excellent high DC voltage gain. In addition, this technique reduces current stresses in the power electronic switching devices that lead to low conduction losses [10]–[11], however, the issue of ripple current may rise as  $D$  decreases.

This research paper proposes a circuit topology that

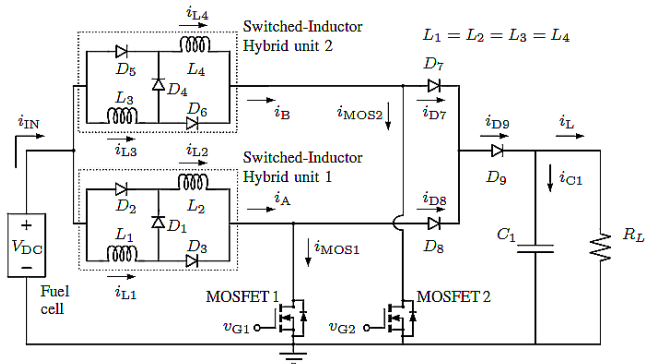


Fig. 1. The proposed interleaved switched-inductor hybrid DC boost circuit.

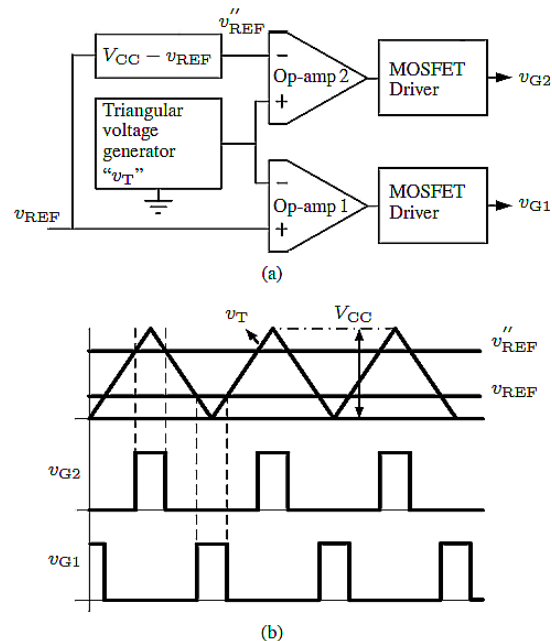


Fig. 2 Generation of the duty cycle signal. (a) control circuit scheme. (b) the timing waveforms.

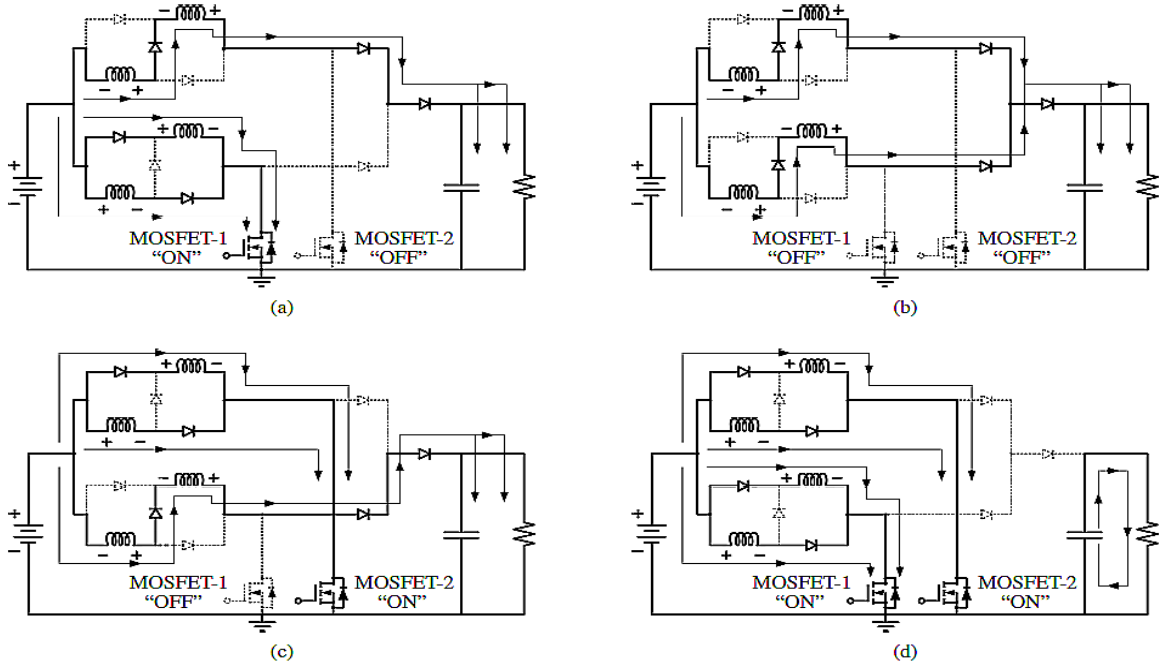


Fig. 2 Various operating modes along with current-flow path, of the of the proposed switch-inductor hybrid DC converter. (a) Mode 1. (b) Mode 2. (c) Mode 3. (d) Mode 4

interleaves two switched-inductor hybrid units. The merit of using the switched-inductor hybrid unit is that it provides a DC voltage gain to the load. Whereas, the merit of interleaving includes ripple current reduction, whereas another merit is that additional switched-inductor hybrid units can be interleaved, and the circuit may be expanded. It is understood that by interleaving additional switched-inductor hybrid units, the ripple current may further decrease. Such a technique may aid in reducing the filter capacitor size. The scope of this research paper is to demonstrate the interleaving of only two switched-inductor hybrid units.

## 2. INTERLEAVED SWITCHED-INDUCTOR HYBRID DC BOOST CONVERTER

Fig. 1 displays the proposed interleaved switched-inductor hybrid DC boost converter circuit. A fuel cell is connected to two switched-inductor hybrid units, where switched-inductor hybrid unit number 1 consists of inductors  $L_1$  and  $L_2$  and fast-switching diodes  $D_1$ ,  $D_2$ , and  $D_3$ . Similarly, switched-inductor hybrid unit number 2 consists of inductors  $L_3$  and  $L_4$  and the fast-switching diodes are  $D_4$ ,  $D_5$ , and  $D_6$ . Switched-inductor hybrid unit number 1 and 2 are interleaved by the help of MOSFET's -1 and -2, respectively. Diodes  $D_7$  and  $D_8$ , and  $D_9$ , are used as reverse current blocking diodes. Whereas  $C_1$  is a filter capacitor and  $R_L$  is the load resistance. It is assumed the inductors  $L_1$ ,  $L_2$ ,  $L_3$ , and  $L_4$ , have identical symmetry and value.

### 2.1 Generation of Control Sequence

Fig. 2(a) displays the control scheme where a function generator generates a triangular voltage waveform,  $v_T$ .

This triangular voltage is fed to the inverting terminal of operational amplifier (op-amp) 1 and to the non-inverting terminal of op-amp 2. Both op-amps are being used as comparators. The non-inverting terminal of op-amp 1 is provided with the reference voltage  $v_{REF}$ . The inverting terminal of op-amp 2 is provided with a modified reference voltage  $v_{REF}'$ , given as

$$v_{REF}' = V_{CC} - v_{REF} \quad (1)$$

Where  $V_{CC}$  is the peak voltage of triangular voltage waveform as shown in Fig. 2(b). The outputs of op-amps -1 and -2 are connected to separate commercial MOSFET drivers such as model IR2110 manufactured by International Rectifier<sup>TM</sup>. The output voltage signals of individual drivers, i.e.,  $v_{G1}$  and  $v_{G2}$ , drive the gate-terminals of MOSFET-1 and -2, respectively.

### 2.2 Working of a Switched-Inductor Hybrid Unit

Depicted in Fig. 1, the working of a switch-inductor hybrid unit will be presented. For example, as MOSFET-1 is switched ON inductor  $L_1$  is energized through  $D_3$ , and  $L_2$  is energized through  $D_2$ . The voltage polarity appearing across inductors  $L_1$  and  $L_2$  are the same as of the fuel cell voltage,  $V_{DC}$ , under such condition the inductors appear in parallel configuration. If  $i_{L1}$  is the current in  $L_1$ , and  $i_{L2}$  is the current in  $L_2$ , since the inductors are in symmetry, then

$$i_{L1} = i_{L2} = \frac{V_{DC}}{L_1} (t_2 - t_1) \quad (2)$$

where  $t_1$  and  $t_2$  represent the starting and ending time of mode-1, respectively.

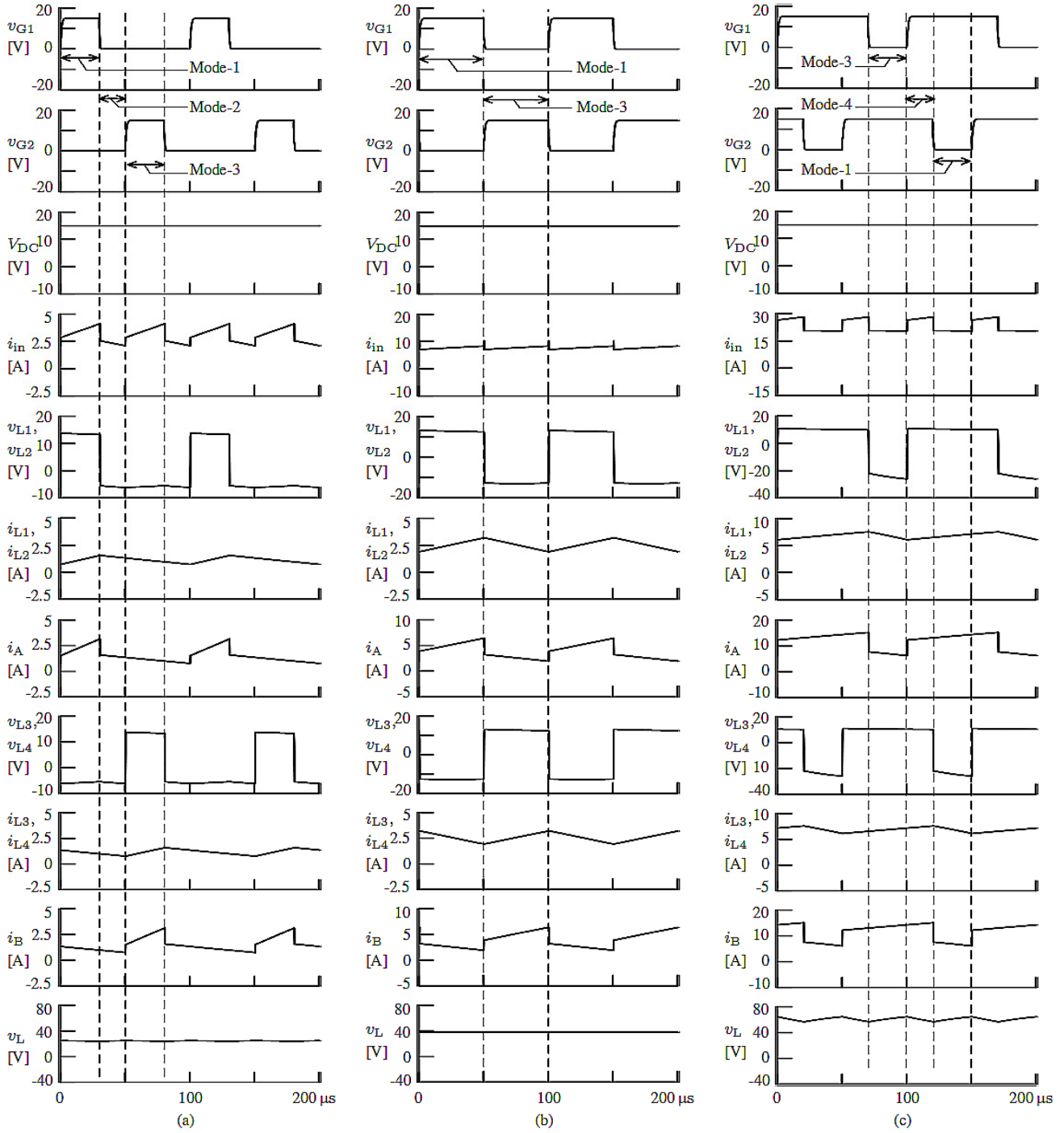


Fig. 3 Simulated response of the proposed switched-inductor hybrid DC converter (a) for  $D=0.3$  (b) for  $D=0.5$  (c) for  $D=0.7$

However, when MOSFET-1 is switched OFF, the voltage polarity of inductors  $L_1$  and  $L_2$  reverses in direction. The reverse polarity across inductors  $L_1$  and  $L_2$  reverse bias diodes  $D_2$  and  $D_3$ , respectively. With  $D_2$  and  $D_3$  reversed biased, the current flowing in  $L_1$  flows through and  $D_1$  and then through  $L_2$ . Therefore, inductors  $L_1$  and  $L_2$  become a series circuit. Assuming a zero voltage drop across a conducting diode, the voltage appearing across the load,  $v_L$ , is expressed as,

$$v_L = V_{DC} + v_{L1} + v_{L2} \quad (3)$$

### 2.3 Working of the proposed circuit

With reference to Fig. 1, the steady state analysis of the proposed interleaved switched-inductor hybrid DC converter is described in the following four modes. It should be noted that both MOSFETs have same turn-on and turn-off times.

Mode-1: Fig. 3(a) demonstrates the instant when MOSFET-1 is turned ON and MOSFET-2 is OFF. Inductors  $L_1$  and  $L_2$ , of

switched-inductor hybrid unit 1, appear in parallel configuration and are charged with a constant voltage. For the switched-inductor hybrid unit 2, since MOSFET-2 is turned, the inductors  $L_3$  and  $L_4$  appear in series configuration. The voltage stress observed at source-terminals of MOSFET-2 is essentially equal to the output load voltage.

Mode-2: Fig. 3(b) demonstrates the instant when both MOSFET-1 and -2 are turned off. The inductors of switched-inductor hybrid unit 1 are now in series configuration. Similarly, the inductors of switched-inductor hybrid unit 2 are now also in series configuration. In this mode inductors of both switched-inductor

Parameter	D = 0.3		D = 0.5		D = 0.7		Unit
	Min.	Max.	Min.	Max.	Min.	Max.	
$i_{IN}$	2.1	4.12	7	10.27	20.37	28.13	A
$v_{L1}, v_{L2}, v_{L3}, v_{L4}$	-6.2	13.78	-13	13	-26.12	10.7	V
$i_{L1}, i_{L2}, i_{L3}, i_{L4}$	0.75	1.56	1.93	3.24	6.1	7.54	A
$v_{D2}, v_{D3}, v_{D5}, v_{D6}$	-5.33	0.86	-12.13	0.86	-25.24	0.91	V
$v_{MOS1}, v_{MOS2}$	0.43	26.51	1.1	40	3.38	66.34	V
$i_{MOS1}, i_{MOS2}$	-0.1	3.13	-0.1	6.4	-0.1	15.08	A
$v_L$	23.4	24.8	37.5	38.4	56.44	64.58	V
$i_L$	1.56	1.65	2.5	2.5	3.76	4.3	A
$i_{CI}$	-0.6	1	0.8	2.56	-4.3	3.85	A

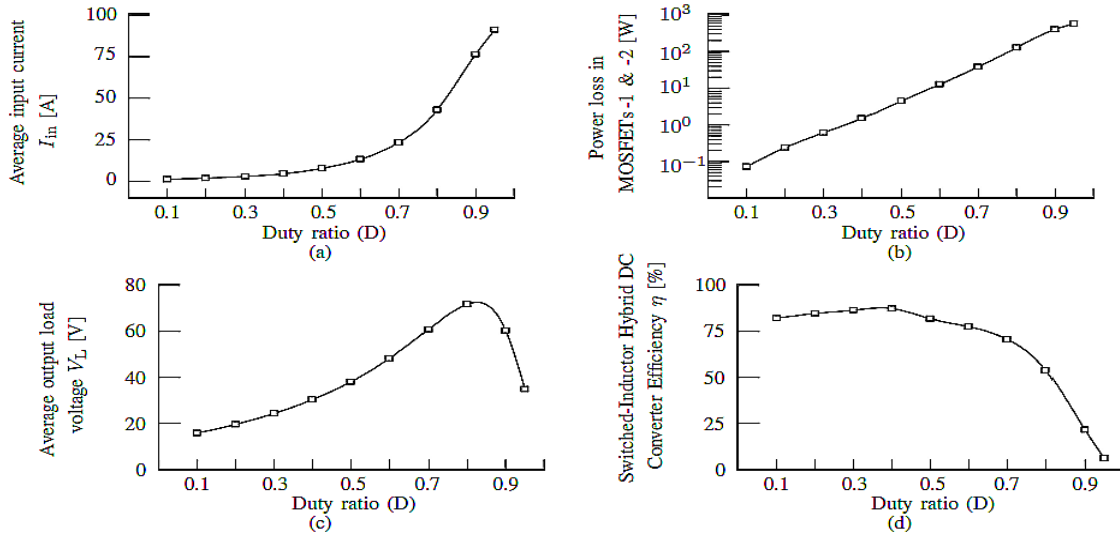


Fig. 4 Simulated performance of various parameters of the proposed switch-inductor hybrid DC converter circuit as D ranges from 0 to 1 (a) shows the average input current (b) shows the power dissipation in MOSFETs -1 and -2 (c) shows the average output load voltage (d) shows the efficiency

hybrid units are essentially discharging via the load. The voltage stress observed at source-terminals of both MOSFETs is essentially equal to the output load voltage.

Mode-3: Fig. 3(c) demonstrates the instant when MOSFET-1 is turned off and MOSFET-2 is on. For the switched-inductor hybrid unit 1, the inductors  $L_1$  and  $L_2$  appear in series configuration. The voltage stress observed at source-terminal of MOSFET-1 is essentially equal to the output load voltage. Inductors  $L_3$  and  $L_4$ , of switched-inductor hybrid unit 2, appear in parallel configuration and are charged with a constant voltage, i.e.,  $V_{DC}$ .

Mode-4: Fig. 3(d) demonstrates the instant when MOSFETs-1 and -2 are both turned on. In this mode, all inductors of switched-inductor hybrid unit 1 and 2 appear in parallel configuration, and are in charging state. During this mode-4, since the diodes  $D_7$ ,  $D_8$ , and  $D_9$ , are reversed biased, therefore, the capacitor  $C_1$  discharges through the load resistor.

Table 2. Proposed Interleaved Switched-Inductor Hybrid Dc Boost Converter Maximum And Minimum Voltage And Current Values For Various D Kept Equal To 0.3, 0.5, And 0.7

### 3. SIMULATED RESULTS

The proposed interleaved switched-inductor hybrid DC converter circuit is simulated using Proteus Virtual System Modeling (VSM)™ software from Labcenter Electronics™. Proteus VSMTM had been selected as it routines mixed mode SPICE1 circuit simulations. SPICE abbreviates for Simulation Program with Integrated Circuit Emphasis.

With reference to Fig. 1, the circuit parameters are set as follows; input voltage  $V_{DC}=15V$ , inductors  $L_1, L_2, L_3$ , and  $L_4 = 500\mu H$  each, capacitor  $C_1 = 10\mu F$  (polarized capacitor), diodes  $D_1$  to  $D_9$  are fast switching diodes (e.g., model number SUF15J), both MOSFETs -1 and -2 were IRFP460, whereas  $R_L=15\Omega$ . These circuit parameter were so selected that the converter operates in continuous conduction mode (CCM).

The control signals for driving the MOSFETs-1 and -2 as shown in Fig. 2, were generated by setting the frequency of the triangular voltage waveform to 10kHz, and a peak voltage,  $V_{CC} = 10V$ . As indicated in the figure, the duty cycle is variable from 0 to 1. The reference voltage,  $v_{REF}$ , was variable from 0 to 10 V.

**1) Results for  $D = 0.3$  ( $D < 0.5$ ):** Fig. 4(a) displays the voltage and current waveforms of the proposed interleaved switched-inductor hybrid DC boost converter for  $D = 0.3$ . Only mode-1, -2, and -3, are present whereas mode-4 is absent. For an input voltage of 15V, the minimum and maximum voltage and current values of various circuit components are summarized in Table I. Such a summary may also be useful in determining thermal

properties of electronic components in the circuit. The observed average DC output voltage is approximately equal to 24 V.

**2) Results for  $D = 0.5$ :** Fig. 4(b) displays the voltage and current waveforms of the proposed interleaved switched-inductor hybrid DC boost converter for  $D = 0.5$ . Only mode-1 and -3, are present whereas mode-2, and -4 are absent. For an input voltage of 15V, the minimum and maximum voltage and current values of various circuit components are summarized in Table I. The observed average DC output voltage is approximately equal to 38V.

**3) Results for  $D = 0.7$  ( $D > 0.5$ ):** The simulated voltage and current waveforms of the interleaved switched-inductor hybrid DC boost converter for  $D = 0.7$ , are presented in Fig. 4(c). Only mode-1, -3, and -4 are present whereas mode-2 is absent. For an input voltage of 15V, the minimum and maximum voltage and current values of various circuit components are summarized in Table I. The observed average DC output voltage is approximately equal to 60V, whereas the peak-to-peak output ripple voltage is observed to be 8V.

#### 4. DISCUSSION

A careful examination of Fig. 4 indicates that for a given value of  $D$ , the proposed interleaved switched-inductor hybrid DC boost converter operates only in three modes of operation. When  $D$  is kept less than 0.5, e.g., as in Fig. 4(a) (mode-1, -2, and -3 are present whereas mode-4 is absent), in this condition ( $D < 0.5$ ), the capacitor  $C_1$  charges in mode -1 and -3 while it discharges in mode -2. However, the condition  $D = 0.5$  is an exception where the proposed converter operates only in mode-1 and -3. When  $D = 0.5$ , as in Fig. 4(b), the capacitor  $C_1$  charges and discharges in the same mode. Whereas, for  $D > 0.5$ , e.g., in Fig. 4(c), only mode-1, -3, and -4 are observed. In this condition ( $D > 0.5$ ), the capacitor  $C_1$  charges in mode -1 and -3 while it discharges in mode -4.

Observations of average input current, power-dissipation in MOSFET-1 (also applicable to MOSFET-2), output load voltage, and efficiency of the proposed converter, as a function of  $D$  are presented in Fig. 5. Fig. 5(a) displays that the input current increases exponentially as  $D$  increases. For a value of  $D$  beyond 0.7 the input current becomes excessive large. This can be explained as follows. The input current is consumed only at the time when MOSFETs-1 or -2 are switched on (at their respective time), for values of  $D$  less than 0.5, since this the switching time of MOSFETs is small as compared to turn-off time therefore the input current is consumed less. However, as  $D$  increase beyond 0.5, the MOSFET turn-on time exceeds the turn off time and thereby, causing more current to be consumed from the source. Fig. 5(b) indicates the consequences of increasing the input current is faced by the MOSFETs in the form of large dissipation loss and large stress voltage (also Table I). Fig. 5(c) suggests that the load voltage of proposed interleaved switched-inductor hybrid DC boost converter may be considered linear for  $D$  ranging from 0 to 0.6. An interesting observation is regarding the efficiency of the proposed converter as shown in Fig. 5(d). The simulated results indicate that the proposed converter shows highest efficiency of 85 % for  $D = 0.4$ .

#### 5. CONCLUSION

The main contribution of this research is to put forward a model of the interleaved switched-inductor hybrid DC converter. Results have shown that the proposed interleaved switched-inductor hybrid DC converter shows stability for duty ratio ranging from 0.1 to 0.7. The proposed converter can operate in

four-modes with the help of interleaved switching technique. The main advantage of the proposed converter is the lower stored energy in the magnetic elements, which leads to less weight, size and cost reduction for the inductors. As more switched-inductor hybrid units are interleaved the filter capacitor size can be reduced. Simulated results of the proposed converter substantiate the performance of the design system.

#### 6. REFERENCES

- [1] W. Li, Y. Zhao, Y. Deng, and X. He, "Interleaved converter with voltage multiplier cell for high step-up and high-efficiency conversion," *IEEE Trans. Power Electron.*, Vol. 25, No. 9, Sept. 2010, pp. 2397–2408.
- [2] Muhammad H. Rashid, "Power Electronics: Circuits, Devices and Applications," *Prentice Hall, 3ed.*, Aug. 14, 2003, pp.176–177.
- [3] M. Prudente, L. L. Pfitscher, G. Emmendoerfer, E. F. Romaneli, and R. Gules "Voltage multiplier cells applied to non-isolated DCDC converters," *IEEE Trans. Power Electron.*, Vol. 23, No. 2, March 2008, pp. 871–887.
- [4] Q. Zhao, and F. C. Lee "High-efficiency, high step-up dc-dc converters," *IEEE Trans. Power Electron.*, Vol. 18, No. 1, Jan. 2003, pp. 65–73.
- [5] W. Li, and X. He, "Review of nonisolated high-step-up dc/dc converters in photovoltaic grid-connected applications," *IEEE Trans. Ind. Electron.*, Vol. 58, No. 4, April 2011, pp. 1239–1250.
- [6] P. Lee, Y. Lee, D. Cheng, and X. Liu, "Steady-state analysis of an interleaved boost converter with coupled inductors," *IEEE Trans. Ind. Electron.*, Vol. 47, No. 4, Aug. 2000, pp. 787–795.
- [7] G. Calderon-Lopez, A. J. Forsyth, and D. R. Nuttall, "Design and performance evaluation of a 10-kW interleaved boost converter for a fuel cell electric vehicle," *Proc. IEEE Power Electron. Motion Control Conf.*, Aug. 2006, Vol. 2, pp. 1-5.
- [8] P. Thounthong, and S. Pierfederici "A new control law based on the differential flatness principle for multiphase interleaved DC-DC converter," *IEEE Trans. Circuits Syst-II: Express Briefs*, Vol. 57, No. 11, Nov. 2010. pp. 903–907.
- [9] J. Lee, Y. Jeong, and B.Han "An isolated dc/dc converter using high-frequency unregulated LLC resonant converter for fuel cell applications," *IEEE Trans. Ind. Electron.*, Vol. 58, No. 7, July 2011, pp. 2926–2934.
- [10] B. Axelrod, Y. Berkovich, and A. Ioinovici, "Switched-capacitor/switched-inductor structures for getting transformerless hybrid DC-DC PWM converters," *IEEE Trans. Circuits Syst-I: Reg. Papers*, vol. 55, no. 2, pp. 687–696, Mar. 2008.
- [11] L. S. Yang, T. Liang, and J. Chen, "Transformerless DC-DC converters with High step-up voltage gain," *IEEE Trans. Ind. Electron.*, Vol. 56, no. 8, Aug. 2009. pp. 3144–3152.

\*\*\*\*